Self-rectifying threshold resistive switching based non-volatile memory of CBD/CBD grown vertical n-ZnO nanowire/p-Si heterojunction diodes

Rajib Saha, Avishek Das, Anupam Karmakar, Sanatan Chattopadhyay*

Department of Electronic Science, University of Calcutta, Kolkata 700009, India.

*Corresponding author

DOI: 10.5185/amp.2018/836
www.vbripress.com/aml

Abstract

Vertically oriented ZnO nanowires are grown on p-Si substrate by employing two-step sequential chemical bath deposition technique. The ZnO nanowire exhibits n-type doping due to the presence of oxygen vacancies. The electrical characterizations of n-ZnO NWs/p-Si heterojunction diodes exhibit a self-rectifying, threshold resistive switching behavior. Such switching behavior is explained by oxygen vacancy assisted conducting filament formation mechanism. The relevant charge transport is governed by TC-SCLC and multistep recombination-tunneling processes through the interface traps. Threshold-voltage for resistive switching is observed to be increasing with increasing bias sweep rate. The device shows superior memory endurance for forward and reverse voltage sweep of 50 cycles in fast sweep mode. The ratio of HRS to LRS resistances shows one order of difference. The retention time of such resistive switching memory is recorded to be 4000 seconds, suggesting its non-volatile functionality. Thus, the n-ZnO NWs/p-Si heterojunction can be employed for fabricating promising non-volatile memory devices with excellent endurance and retentions.

Keywords: ZnO nanowires, n-ZnO NWs/p-Si heterojunction, threshold resistive switching memory, oxygen vacancy, conducting filament formation.

Introduction

Resistive switching property of semiconductor materials has gained enormous scientific and industrial interest due to its capability of fabricating functional memory devices **[1–3]**. Such devices are projected to be the next generation memory components due to its cost effectiveness, non-volatility, fast-switching, high ON/OFF switching ratios, high endurance and retentions **[4]**. Several research groups have proposed a number of binary metal oxides for resistive switching memory applications including ZrO_2**[5]**, Al_2O_3**[6]**, ZnO **[7–9]**, TiO_2**[10]** and NiO**[11]**. Among these, zinc oxide (ZnO) nanowire is one of the most attractive materials for resistive switching applications due to its high transparency to visible light, high surface-to-volume ratio, 1- dimensional (1-D) charge transport and cost-effective technology **[12]**. The ZnO nanowires are intrinsically n-type in nature due to the presence of oxygen vacancy related defects, which also acts as traps in the bulk and at the interface **[13]**. Several techniques have been reported for the growth of superior quality ZnO nanowires (NWs) including chemical vapor deposition (CVD) **[14]**, vapor-liquid-solid (VLS) method **[15]**, molecular beam epitaxy (MBE) **[16]**, sputtering **[17]**, sol-gel **[18]** and chemical bath deposition (CBD) **[19,20]** process. Among these techniques, the CBD method is a superior choice for low temperature, bottom-up growth of the vertically aligned ZnO NWs. Still there are many reports available which claims the cost-effective, rapid growth of ZnO nanostructures by employing seed assisted CBD technique **[21,22]**. However, such techniques require expensive equipments such as spin-coater, annealing furnace for ZnO seed preparation on substrate, which ultimately lead to expensive cost-of-fabrication of nanowire devices. In this context, double step CBD/CBD technique can be employed for ZnO nanowire growth, where both the ZnO seeds and nanowires can be grown by CBD technique itself **[20,23]**. For the wide application of memory devices including in digital electronics, uni-directional (current-voltage in 1st quadrant) resistive memory is more favorable in comparison to their bi-directional counter part due to the self-rectification, simplified circuit design and fabrication technology. This self-rectification of the switching can be achieved by growing defect doped n-ZnO NWs directly on the p-Si substrate by employing CBD technique **[20,24]**. Moreover, the intrinsic defects such as oxygen ions and vacancies in n-ZnO nanowire are extremely important for the formation of conductive filament along the nanowire

c-axis, which is the fundamental switching mechanism known till date **[7–9,25]**. These defects are reported to be mobile under biasing conditions and the relevant filament formation depends on various properties such as time of bias sweep, defect activation energy, filament temperature **[1,26,27]**. Thus, the investigation of resistive switching mechanism in presence of intrinsic defects in ZnO NW is essential in order to develop a comprehensive understanding on the memory effect of n-ZnO/p-Si heterojunction.

In the current work, the vertically aligned ZnO nanowires are grown on p-Si substrate by employing chemical bath deposition method (CBD/CBD). Prior to the growth of nanowires, a ZnO seed layer is grown also by CBD process. The material characterizations have been performed to study the defects in the ZnO NWs. The resistive switching performance of the n-ZnO NWs/p-Si heterojunction diodes is studied by measuring the relevant current-voltage (I-V) characteristics. The resistive switching kinetics is investigated by applying the filament formation theory and energy-band diagram. The effect of bias sweep rate on the threshold-voltage/ set-voltage has been studied in order to overcome the voltage-time dilemma. Endurance of such memory devices are tested by 50 continuous loops of I-V measurement. Moreover, a retention test is also performed to measure the device reliability by applying constant voltage stress.

Experimental

For the growth of ZnO nanowires, standard <100> p-type silicon (Si) substrate has been used. The Si substrate is cleaned sequentially with trichloroethylene, acetone and iso-propyl alcohol sequentially for 5 min under ultrasonication. The cleaned substrate is sensitized with ZnO nano-particle seed prepared by employing CBD/CBD method [20], where the substrate is dipped in an aqueous solution of 50 mM of zinc nitrate hexahydrate ($Zn(NO_3)_2.6H_2O$) followed by addition of ~1 ml of ammonia solution (NH4OH). The ZnO seeds are grown for 30 min with a constant bath temperature of 90 ^oC. Further, the seed prepared sample is dipped in the bath solution containing equi-molar aqueous solutions of 50 mM of zinc nitrate hexahydrate and hexamethylenetetramine ($C_6H_{12}N_4$) for ZnO nanowire growth. The bath solution is heated to 90 ^oC and growth is performed 2 hours. After the growth, the nanowire sample is rinsed in DI water and dried by blowing N_2 gas.

The structural morphology of the CBD/CBD grown ZnO nanowires is studied by using a JEOL field emission scanning electron microscope (FESEM) JSM 6700F. Crystallographic study of the grown nanowires is performed by using x-ray diffraction (XRD). Cathodoluminescence (CL) and X-ray photoelectron spectroscopy (XPS) are carried out to investigate the presence of intrinsic defects in the grown ZnO nanowires. Ohmic contacts are formed by using thermally evaporated Al on the back-side of p-Si substrate and Ag on top-side of the n-ZnO nanowires. The bias voltage is applied to p-Si substrate whereas n-ZnO side is electrically grounded. The electrical measurements are performed by using Keithley 4200 SCS semiconductor parameter analyzer connected in the Cascade Microtech-1200Mprobe station.

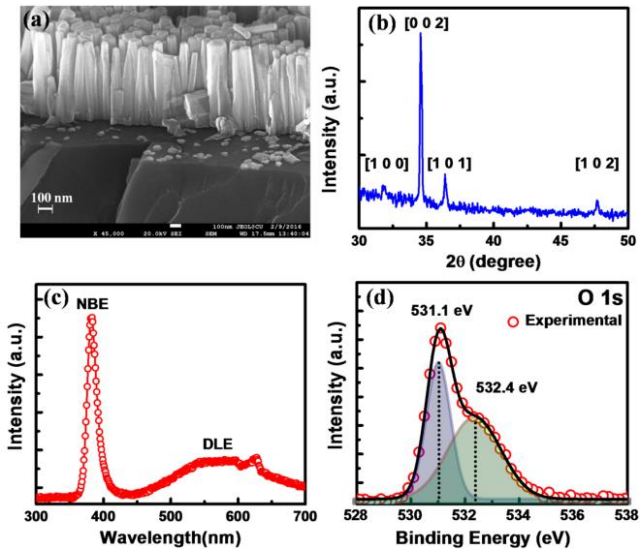

Fig. 1. (a) Cross-sectional FESEM image of ZnO nanowires on Si; (b) corresponding X-ray diffraction pattern; (c) Cathodoluminescence spectra; and (d) X-ray photoelectron spectroscopy profile for O 1s.

Results and discussion

Fig. 1(a) shows the growth of highly dense ZnO nanowires on Si substrate by employing double-step CBD technique. It is evident from such figure that the grown ZnO nanowires acquire regular hexagonal facets and are highly vertically oriented. Such vertically oriented nanowires show the significance of using ZnO nanoparticle seeds which acts as template for nanowire growth. The average diameter and height of such nanowires are measured to be 190 nm and 1.4 μm, respectively.

This vertical growth of ZnO nanowires is also evident in the X-ray diffraction pattern obtained in **Fig. 1(b),** which clearly depicts the formation of poly-crystalline ZnO crystals. The dominant diffraction peak for [002] plane originating at $2\theta = 34.56^o$ confirms the c-axis growth of hexagonal wurtzite ZnO nanowires. The existence of defects in ZnO NWs is characterized by employing room-temperature cathodoluminescence (CL) spectroscopy which is shown in **Fig. 1(c).** The CL spectra reveal a sharp near-band edge (NBE) emission originating at 380 nm which corresponds to the recombination of excitons with ZnO band gap. Moreover, a broad green-yellow deep level emission centered at ~550 nm is attributed to the presence of oxygen vacancy in ZnO NWs **[28]**. It is well known that the oxygen vacancies are not only responsible for generating donor doping, however, it also acts as deep level traps inside the bandgap of ZnO **[13,28–30]**. In order to visualize the presence of oxygen related defects, X-ray photoelectron spectroscopy (XPS) is performed for O 1s chemical state and plotted in **Fig. 1(d).** The XPS spectra shows an aysmmetric peak which is deconvoluted into two gaussian components with

binding energy peaks centered at 531.1 eV and 532.4 eV. The peak corresponding to 531.1 eV indicates the presence of O^{2-} ions in oxygen-deficient regions, which is corroborated with the CL-DLE peak for oxygen vacancy in ZnO depicted in **Fig. 1(c).** Moreover, the peak originating at 532.4 eV is associated with the chemisorbed oxygen species at the nanowire surface during the chemical solution growth process **[29]**.

For the electrical characterizations of such oxygen vacancy induced n-doped ZnO NWs/p-Si heterojunction diode, ohmic contact to Si is formed by depositing Al metal. The electron affinity of p-Si and n-ZnO are 4.05 eV and 4.50 eV [**20,24**], respectively, whereas the work function of Ag is 4.26 eV, which confirms the formation of a good ohmic contact with n-ZnO NWs. Due to the relatively higher valence band offset (ΔE_V = 2.7 eV) than the conduction band (ΔE_C= 0.45 eV), the charge transport over the heterojunction barrier is reported to be dominated by electrons [**20**].The effective contact area is measured to be ~2.1×10^{-3} cm^2 which covers approximately 10^6 ZnO nanowires (NWs). The contact to n-ZnO NWs is electrically grounded and relative bias is applied to p-Si substrate, as shown at the inset of **Fig**. 2(a). The bias at p-Si side is swept in a cyclic fashion from -15 V→0 V →+15 V→0→-15 V, and the corresponding current-voltage characteristics are shown in **Fig. 2(a).**

The characteristics show a rectifying behaviour of donor doped ZnO NWs/p-Si with a current hysteresis loop in forward bias regime. In the first voltage sweep cycle, when the applied voltage reaches to ~ 11.9 V, the current of the device increases rapidly from 4.38 mA to 34.21 mA, thereby indicates that the diode achieves electrical transition from high resistance state (HRS) to low resistance state (LRS) leading to "ON" state. Similar switching characteristics have been reported which claims such interesting behavior as 'Threshold resistive switching' **[25,31–33]**. Such an abrupt increase of current at 11.9 V (threshold / set voltage) is attributed to the electroforming process of conducting filament inside ZnO **[9,34]** and consequently the device is switched to LRS (ON) state. When the bias is swept back to a particular voltage (hold / reset), a sudden decrease in current occurs and the conductance state switches back to HRS from LRS and an "OFF" state is achieved. Moreover, the diode shows the resistive memory behavior only in the forward bias regime, thereby exhibits a uni-directional resistive switching behavior due to the self-rectifying property of n-ZnO NWs/p-Si heterojunction. In order to study the charge transport mechanism of such threshold resistive switching in the heterojunction, the experimental I-V data are fitted with several known conduction modes and plotted in **Fig. 2(b).** The log I - log V characteristics during forward sweep in **Fig. 2(b)** depicts three different slopes suggesting different conduction mechanisms. The conduction mechanism in lower voltage region (<1 V) exhibits a linear current-voltage characteristics with a slope S_1 of 1.3 confirming ohmic transport (IαV). However at higher biases, the slope S_2 and S_3 is ~ 2, which signifies trap-controlled space charge limited current (TC-SCLC) transport ($I \alpha V^2$). Similar result has

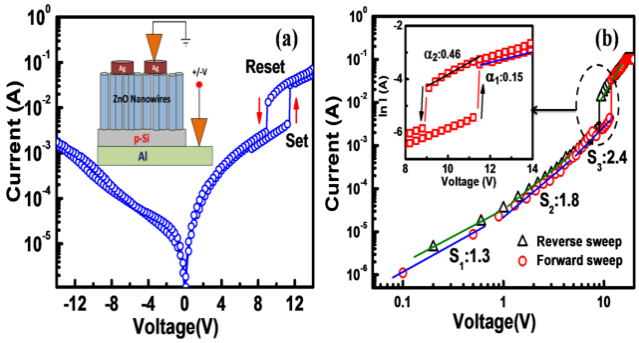

Fig. 2. (a) Current-voltage characteristics of n-ZnO NWs/p-Si heterojunction diode at forward and reverse bias sweep. Inset shows the schematic for electrical measurement setup; (b) Log (I)-log (V) plot of current-voltage characteristics of the n-ZnO NW/p-Si heterojunction diode. Inset shows the log I-V plot in the voltage range 8 V to 14 V.

also been found for ZnO thin film based resistive switching devices grown by atomic layer deposition technique **[7]**.Such TC-SCLC transport can be attributed to the presence of oxygen vacancies in the ZnO NWs, which has been confirmed by CL and XPS results in **Fig. 1(c-d).** For investigating the charge transport during ON state, the Log I-V characteristics is plotted and shown in the inset of **Fig. 2(b).** The characteristics show that after the threshold / set voltage, the slope α_1 is 0.15 V^{-1} and while reverse sweeping of voltage below its threshold value, the slope α_2 is recorded to be 0.46 V^{-1}. This depicts that the charge transport after threshold voltage is dominated by multistep recombination-tunneling mechanism through interface traps between n-ZnO NWs/p-Si junction. The corresponding current-voltage relation is given by I α exp (αV) which is usually observed in wide-band gap semiconductor [**24,35**]. Similar result has also been reported for CBD grown single standalone n-ZnO nanowire/p-Si heterojunction diode, where at higher bias voltage the dominant transport is observed to be multistep recombination-tunneling mechanism [**24**].

The formation of conductive filament and its rupture are the most probable mechanism of such threshold resistive switching process. This mechanism can be explained in terms of energy band diagram at the relevant bias voltages which is depicted in **Fig**. **3(a-d).** It can be observed from **Fig**. **3(a)** that under no bias the oxygen ions are randomly distributed over the entire length of ZnO nanowire, which is responsible for donor doping. In **Fig**. **3(b),** under the forward bias below threshold (V_{th}/ V_{set}), these oxygen ions are migrated due to the application of an external electric field and more oxygen-vacancy related doping are generated. This enhanced doping generates more electrons in the conduction band (C.B.) of n-ZnO as depicted in the energy-band diagram of **Fig. 3(b).** With positive voltage sweep, the oxygen ions (O^{2-}) migrate from ZnO NWs to n-ZnO NWs/p-Si interface, thereby, leaving behind the oxygen vacancies in the nanowires. Such oxygen vacancy related defects gather and aligns along the c-axis of the individual nanowires to form tiny conducting filaments at HRS condition. At V_{th}, the entire conducting filament is formed

and the current increase abruptly leading to LRS and the device is switched to SET condition, which is depicted in **Fig. 3(c).** At and above V_{th}, the electrical charges are transported through the interface traps by multistep recombination and tunneling mechanism as shown in the energy-band diagram of **Fig. 3(c).**

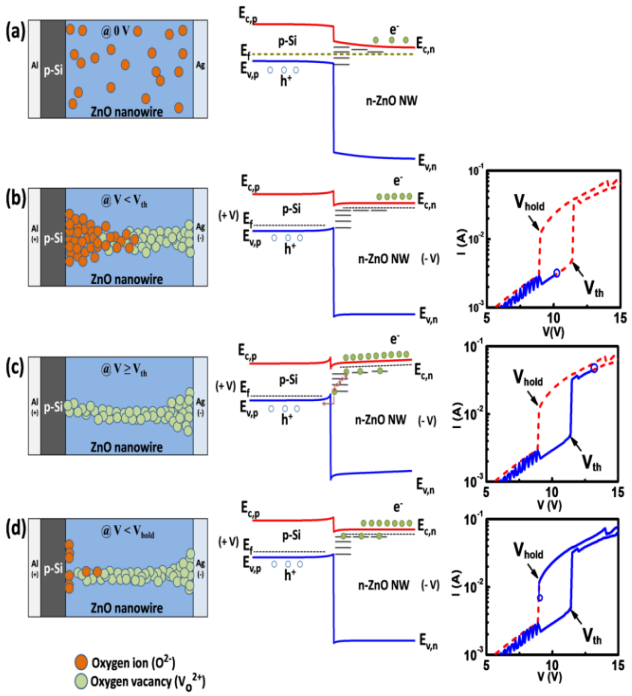

Fig. 3. (a-d) Schematics of filament formation, relevant energy band diagram and I-V characteristics for threshold resistive switching memory operation of n-ZnO NWs/p-Si heterojunction diode at different forward bias voltages (doted line shows the actual switching operation path and solid line shows the state of current at the given voltage).

During the RESET process shown in **Fig**. 3(d), the relative electric field is in reverse direction i.e., from n-ZnO NW side to p-Si side. The oxygen ions near the p-Si (virtual electrode) are pushed back to the ZnO nanowire, which neutralizes the oxygen vacancies by recombination process [**7**] and hence the effective concentration of electrons decreases in the C.B. of n-ZnO NWs. Therefore, at a critical bias V_{hold} / V_{reset} the conducting filament breaks and the device current switches down to HRS as depicted in **Figs. 2** and **3**.

In order to correlate the kinetics of filament formation process to switching mechanism, the forward current-voltage characteristics of the heterojunction diode is measured with different sweep rates such as the fast (0.1 V/7.8 ms), normal (0.1 V/25.46 ms) and quiet (0.1 V/93.45 ms) modes and the relevant threshold-voltages (V_{th}) are extracted. The current-voltage (I-V) characteristics at such modes within the forward voltage regime and V_{th} are shown in **Fig**. **4(a).** Such characteristics show that the V_{th} strongly depends on the bias sweep rate. The inset of **Fig**. **4(a)** depicts the increasing nature of measured V_{th} with applied bias sweep rate.

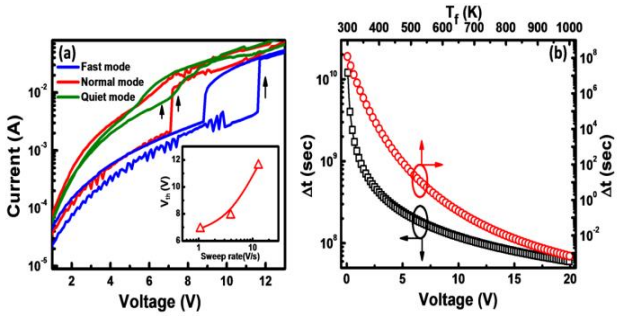

Fig. 4. (a) Plot of switching characteristics of n-ZnO NWs/p-Si diode under various sweep rates (fast, normal and quiet mode) and inset shows the plot of V_{th} with sweep rates; (b) Variation of filament formation time with bias voltage (T_f= 300 K) and filament temperature (V_{th} = 10 V).

Generally, for the resistive switching based memory process, time for filament formation by oxygen vacancies is expected to be a function of the activation energy, and both bias voltage and time [**25,26,36**]. When the applied voltage is slightly higher than V_{th}, the driving power is large enough to form a conductive filament along the NWs c-axis. The time required for filament formation or 'SET' process can be related to the applied voltage and activation energy by the following relation [**26**]:

$$\Delta t = \frac{L_{NW}}{af} exp\left(\frac{E_a}{kT_f}\right)\left[sinh\left(\frac{qa}{2kT_f}\frac{V}{L_{NW}}\right)\right]^{-1} \quad (1)$$

where, E_a is the activation energy for oxygen vacancy which is reported to be ~ 1 eV for ZnO [**37**], f (= 1013 Hz) is the attempt-to-escape frequency [**25**], a (= 0.52 nm) is the lattice constant of c-axis, T_f is the filament temperature, L_{NW} (= 1.4 μm) is the length of nanowires and V is the applied bias for SET and RESET process, respectively.

With the increasing sweep rate of externally applied voltage, oxygen vacancy transport rate also increases which further drifts the vacancies rapidly from high to low concentration region [**26,27**]. Therefore, the current switches to LHS sharply for high bias sweep rate. Under low sweep rate, slow vacancy migration increases the time (Δt) for filament formation which directly leads low V_{th} voltage. Above V_{th}, mobility of oxygen vacancy increases with the increase of activation energy (hence filament temperature) which results in the exponential increment of drifting of oxygen vacancies. Therefore the current rises exponentially rather than a step jump, under normal and quite mode bias sweep as depicted in **Fig. 4(a).** Using Eqn. (1), the time required for filament formation is calculated for a filament temperature of 300 K and plotted with bias voltage in **Fig**. **4(b).** Such plot indicates that the time required for filament formation decreases as the bias voltage for SET and RESET process increases. Even though the bias voltage increases the field-dependent mobility of vacancies, the filament formation time appears to be higher than the experimental result [**25**]. This indicates the involvement of filament joule heating induced thermal enhanced mobility of vacancies. In order to confirm such involvement of joule

heating in the switching kinetics, the formation time is calculated for threshold-voltage of 10 V and plotted with filament temperature as shown in **Fig. 4(b).** Such plot depicts that the estimated time for filament formation is significantly shortened due to the increase of conducting filament temperature inside the ZnO nanowire. The calculated filament formation time for 1.4 μm long ZnO NW, V_{th} = 10 V and filament temperature of 800 K is estimated to be ~10 ms, which is very close to the swept time of 7.8 ms for bias voltage under 'Fast mode' of operation. Therefore, 'Fast mode' of voltage sweep must be chosen as an optimum biasing condition in order to achieve rapid resistive switching in memory devices.

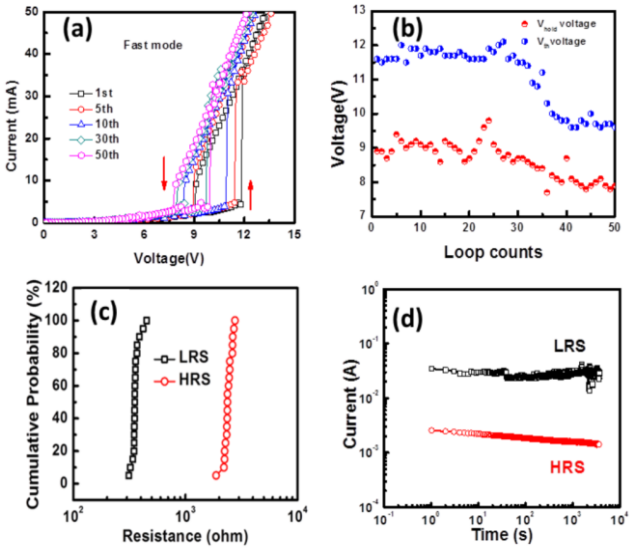

Fig.5 (a) Endurance test of I-V characteristics of the diode under fast mode for 50 voltage sweep cycles; (b) Plot of the variations of set (V_{th}) and reset (V_{hold}) voltages for each memory cycle; (c) Cumulative probability of resistance in HRS and LRS conditions; (d) Current retention test of the fabricated device under 10 V bias stress at room temperature.

The voltage is swept for 50 cycles to testing the device endurance and relevant I-V characteristics are depicted in **Fig**. **5(a).** It is apparent from the plots that the nature of resistive switching memory of n-ZnO NWs/p-Si diode is consistent and thus it indicates non-volatility of such memory devices up to 50 sweep cycles. The variations of V_{th} and V_{hold} voltages with 'Fast mode' bias sweep cycles are shown in **Fig**. **5(b).** Such plot depicts the non-volatile memory nature of the n-ZnO NW/p-Si heterojunction, as the memory window (gap between V_{th} and V_{hold} voltages) is observed to non-overlapping even at 50th sweep cycle. This large memory window is more evident in the cumulative probability plot for the LHS and RHS shown in **Fig. 5(c).** The resistance of the memory switch at HRS is observed to be appearing within 2.68 kΩ to 2.34 kΩ, and its value at LRS are distributed within 328 Ω to 427 Ω. The ratios of high-resistance to low-resistance state (HRS: LRS) are one order of magnitude after the continuous operation of 50 loops in fast-scan mode. Such values of ratio between the HRS and LRS state are significantly high compared to the other reports [**38**]. For evaluating the retention test, a constant voltage stress of 10 V is applied to the device and the relevant variation of current with time is plotted in **Fig. 5(d).** It is apparent from the plot that a retention time more than 4000 seconds at room temperature has been achieved for the device at both HRS and LRS conditions. Based on such results, it is apparent that the CBD grown n-ZnO NWs/p-Si heterojunction can provide uni-directional, self-rectifying stable resistive switching and may be useful for fabricating stable and reliable memory devices for future nano-electronic applications.

Conclusion

Low temperature CBD/CBD technique has been used to grow ZnO nanowires on p-Si substrate to form vertical heterojunction diodes. The average diameter and height of the grown ZnO nanowires are measured to be 190 nm and 1.4 μm. XRD measurements confirm the growth of vertically oriented hexagonal wurtzite ZnO nanowires. Presence of oxygen ions and vacancies are detected by using CL and XPS studies. Such n-ZnO NWs/p-Si heterojunction diodes exhibit a self-rectifying, uni-directional threshold resistive switching memory behavior with a V_{th} of ~11.9 V. The charge transport through the heterojunction is observed to be governed by trap-controlled space charge limited current (TC-SCLC) and multistep recombination-tunneling mechanisms through the interface traps. The mobile oxygen vacancies are found to be highly dependent on the activation energy, bias voltage and bias sweep time and therefore the V_{th} is observed to be increasing with increasing bias sweep rate. The device shows superior endurance for forward and reverse voltage sweep of 50 cycles in fast sweep mode. The variations of V_{th} and V_{hold} voltages with sweep cycles shows non-overlapping memory window which indicate the non-volatile memory behavior of the device. The resistances at HRS and LRS are observed to be appearing within 2.68 kΩ - 2.34 kΩ, and 328 Ω- 427 Ω. The retention time for HRS and LRS conditions are recorded to be 4000 seconds. Thus, the double-step CBD grown n-ZnO NWs/p-Si heterojunction shows self-rectifying behavior with non-volatile resistive switching characteristic of high endurance and retention times which are promising for high density memory development.

Acknowledgements

Mr. Rajib Saha likes to acknowledge the Center of Excellence (COE), TEQIP Phase-II, World Bank (AC/TEQIP-II/CoE/13) for providing the financial support to continue his research work and Mr. Avishek Das likes to acknowledge the University Grants Commission (UGC) (UGC/28/JRF (Upgradation)), India for providing financial support to pursue his research. The authors would also like to acknowledge the DST PURSE program for providing some infrastructural support to conduct this work.

Author's contributions

Conceived the plan: Rajib Saha, Avishek Das; Performed the expeirments: Rajib Saha, Avishek Das; Data analysis: Rajib Saha, Anupam Karmakar, Sanatan Chattopadhyay ; Wrote the paper: Avishek Das, Sanatan Chattopadhyay.

References

1. Menzel,S.; Waters, M.; Marchewka, A.; Bottger, U.; Dittmann, R.; Waser, R.;*Adv. Funct. Mater.*, **2011**, 21, 4487. **DOI:** 10.1016/S1002-0071(12)60001-X
2. Russo, R.; Ielmini, D.; Cagli, C.; Lacaita, A.L.;*IEEE Trans. Electron Devices*., **2009**, 56, 186. **DOI:** 10.1109/TED.2008.2010583
3. Waser, R.; Aono, M.;*Nat. Mater.*, **2007**, 6, 833. **DOI:** 10.1038/nmat2023
4. Kim, K.M.; Jeong, D.S.; Hwang, C.S.;*Nanotechnology*., **2011**, 22, 254002. **DOI:**10.1088/0957-4484/22/25/254002
5. Lin,C.-Y.; Wu,C.-Y.; Wu,C.-Y. ;Tseng,T.-Y. ; Hu,C. ;*J. Appl. Phys*., **2007**, 102, 94101. **DOI:** 10.1063/1.2802990
6. Lin,C.-Y. ; Lee, D.-Y.; Wang,S.-Y. ; Lin, C.-C.; Tseng, T.-Y.;*Surf. Coatings Technol*.,2008, 203, 628. **DOI:**10.1016/j.surfcoat.2008.06.133
7. Zhang, J.; Yang,H., Zhang,Q.; Dong, S.; Luo,J.K.; *Appl. Phys. Lett*., **2013**, 102, 12113. **DOI:**10.1063/1.4774400
8. Chen, C.; Pan, F.; Wang, Z.S.; Yang, J.; Zeng, F.;*J. Appl. Phys.*,**2012**,111. **DOI**:10.1063/1.3672811
9. Chang, W.-Y. ; Lai, Y.C. ; Wu,T.B. ; Wang, S.F.; Chen, F.; Tsai, M.J. ; *Appl. Phys. Lett*., 2008, 92, 022110. **DOI**: 10.1063/1.2834852
10. Acharyya, D.; Hazra, A.; Dutta, K.; Gupta, R.K.; Bhattacharyya, P.; *Semicond. Sci. Technol.*, **2013**, 28, 125001. **DOI**:10.1088/0268-1242/28/12/125001
11. Wang, H.; Zou, C.; Zhou, L.; Tian, C., Fu, D.;*Microelectron. Eng*.,**2012**, 91, 144. **DOI**: 10.1016/j.mee.2011.05.037
12. Wang, Z.L.;*J. Phys. Condenced Matter*., **2004**, 16, R829. **DOI**: http://dx.doi.org/10.1088/09538984/16/25/R01
13. Chicot, G.; Muret, P.; Santailler,J.-L.; Feuillet, G.; Pernot, J.;*J. Phys. D. Appl. Phys.*, **2014**, 47, 465103. **DOI**: 10.1088/0022-3727/47/46/465103
14. Wan, H.; Ruda, H.E.;*J. Mater. Sci. Mater. Electron.*, **2010**, 21, 1014. **DOI**:10.1007/s10854-010-0118-7
15. Li, S.Y.; Lee, C.Y.; Tseng, T.Y.;*J. Cryst. Growth.*, **2003**, 247, 357. **DOI**: 10.1016/S0022-0248(02)01918-8
16. Isakov, I.; Panfilova, M.; Sourribes,M.J.L.; Warburton,P.A.;*Phys. Status Solidi Curr. Top. Solid State Phys.*,**2013**, 10, 1308. **DOI**: 10.1002/pssc.201200940
17. Chiou,W.; Wu, W.; Ting, J.;*Diam. Relat. Mater.*, **2003**, 12, 1841. **DOI**: 10.1016/S0925-9635(03)00274-7
18. Ahn, S.E.; Ji, H.J.; Kim, J., Kim,G.T.; Bae,C.H.; Park, S.M.; Kim,Y.K.; Ha,J.S.;*Appl. Phys. Lett.*, **2007**, 90, 153106. **DOI**: 10.1063/1.2721289
19. McPeak,K.M.; Le, T.P.; Britton, N.G.; Nickolov,Z.S.;Elabd, Y.A.; Baxter,J.B.;*Langmuir*., **2011**, 27, 3672. **DOI**: 10.1021/la105147u
20. Das, A.; Kushwaha, A.; Sivasayan,R.K.; Chakraborty, S.; Dutta, H.S.; Karmakar, A.; Chattopadhyay, S.; Chi, D.; Dalapati, G.K.; *J. Phys. D. Appl. Phys.*, **2016**, 49, 145105. **DOI**: 10.1088/0022-3727/49/14/145105
21. Paul, S.; Das, A.; Palit, M.; Bhunia, S.; Karmakar, A.; Chattopadhyay, S.; *Adv. Mater. Lett.*, **2016**, 7, 610. **DOI**: 10.5185/amlett.2016.6298
22. Dong, J.-J.; Zhen, C.-Y.; Hao, H.-Y.; Xing, J.; Zhang, Z.-L.; Zheng, Z.-Y.; Zhang, X.-W.; Nanoscale Res. Lett., **2013**, 8, 378. **DOI**: 10.1186/1556-276X-8-378
23. Paul, S.; Das, A.; Chakraborty, A.; Chakraborty, B.; Palit, M.; Chattopadhyay, D.; Chattopadhyay, S.; *1st Int. Sci. Technol. Congr*., Elsevier Publications, **2014**, 467.
24. Das, A.; Palit, M.; Paul, S.; Chowdhury, B.N.; Dutta, H.S.; Karmakar, A.; Chattopadhyay, S.;*Appl. Phys. Lett.*, **2014**, 105, 2. **DOI**:10.1063/1.4893944
25. Qi, J.; Olmedo, M.; Zheng,J.-G.; Liu,J.;*Sci. Rep.*,**2013**, 3, 2405. **DOI:** 10.1038/srep02405
26. Menzel, S.; Waters, M.; Marchewka, A.; Bottger, U.; Dittmann, R.; Waser, R.;*Adv. Funct. Mater*.**,2011**, 21, 4487. **DOI**:10.1109/LED.2014.2340016
27. Menzel, S.; Waters, M.; Marchewka, A.; Bottger, U,; Dittmann, R.; Waser, R.;*Adv. Funct. Mater*.,**2011**, 21, 4487. **DOI**:10.1002/adfm.201101117
28. Vempati, S.; Mitra, J.; Dawson, P.; Nanoscale Res. Lett., **2012**, 7, 470. **DOI**:10.1186/1556-276X-7-470
29. Hai-Bo, F.; Shao-Yan, Y.; Pan-Feng, Z.; Hong-Yuan,W.; Xiang-Lin,L.; Chun-Mei,J.; Qin-Sheng, Z.; Yong-Hai, C.; Zhan-Guo, W.;*Chinese Phys. Lett.*, **2007**, 24, 2108. **DOI**: 10.1088/0256-307X/24/7/089
30. McCluskey,M.D.; Jokela,S.J.;*J. Appl. Phys*., **2009**, 106, 1. **DOI**:10.1063/1.3216464
31. Huang,Y.-J.; Chao, S.-C.; Lien, D.-H.; Wen, J.-H. He,C.-Y.; Lee,S.-C.;*Sci. Rep.*, **2016**, 6, 23945. **DOI**: 10.1038/srep23945
32. Nandi,S.K.; Liu,X.; Venkatachalam,D.K.; Elliman,R.G.;*J. Phys. D. Appl. Phys*., **2015**, 48, 195105. **DOI**: 10.1088/0022-3727/48/19/195105
33. Chen, D.;Huang,S.-H.; *Chinese Phys. B.*, 2016, 25, 117701. **DOI**: 10.1088/1674-1056/25/11/117701
34. Seo, J.W.; Park, J.W.; Lim, K.S.; Yang, J.H.; Kang,S.J.; *Appl. Phys. Lett.*, **2008**, 93. **DOI**:10.1063/1.3041643
35. Shi,Z.-F.; Xu,T.-T.; Wu,D.; Zhang,Y.-T.; Zhang,B.-L.; Tian,Y.-T.; Li,X.-J.; Du,G.-T.;*Nanoscale*., **2016**, 8, 9997. **DOI**:10.1039/C5NR07236K
36. Sun, Y.; Yan, X.; Zheng, X.; Liu, Y.; Zhao, Y.; Shen, Y.; Liao, Q.; Zhang, Y.;*ACS Appl. Mater.Interfaces.*, **2015**, 7, 7382. **DOI:**10.1021/acsami.5b01080
37. Oba, F.; Togo, A.; Tanaka, I.; Paier, J.; Kresse, G.;*Phys. Rev. B - Condens. Matter Mater. Phys.*, 2008, 77, 3. **DOI**: 10.1103/PhysRevB.77.245202
38. Chang,W.Y.; Lin,C.A.; He,J.H.; Wu,T.B.;*Appl. Phys. Lett*., **2010**, 96, 242109. **DOI**:10.1063/1.3453450

